Journal of Hydrology 664 (2026) 134553

Contents lists available at ScienceDirect

Journal of Hydrology

journal homepage: www.elsevier.com/locate/jhydrol

Research papers

Numerical investigation of offshore freshened groundwater dynamics in a changing marine environment

Shengchao Yu [a,*], Barret L. Kurylyk [a], Holly A. Michael [b,c], Vittorio Maselli [d,e], Mladen R. Nedimović [d], Irena Schulten [d], Fernando Córdoba-Ramírez [d]

[a] Department of Civil and Resource Engineering and Centre for Water Resources Studies, Dalhousie University, Halifax, Nova Scotia, Canada
[b] Department of Earth Sciences, University of Delaware, Newark, DE, USA
[c] Department of Civil and Environmental Engineering, University of Delaware, Newark, DE, USA
[d] Department of Earth and Environmental Sciences, Dalhousie University, Halifax, Nova Scotia, Canada
[e] Department of Chemical and Geological Sciences, University of Modena and Reggio Emilia, Modena, Italy

ARTICLE INFO

This manuscript was handled by Dongmei Han, Editor-in-Chief, with the assistance of Ryan T. Bailey, Associate Editor

Keywords:
Offshore freshened groundwater
Canadian continental shelf
Onshore-offshore groundwater modeling
Unconsolidated marine sediments
Submarine groundwater discharge

ABSTRACT

Offshore freshened groundwater (OFG) is a potential alternative water resource for coastal populations facing water insecurity caused by high population density, pollution, or converging stressors from atmospheric and oceanic climate change. However, OFG systems are globally less explored than terrestrial groundwater systems, and no prior studies have been conducted on the Canadian continental shelf. Recent observations from two boreholes in the Gulf of St. Lawrence, Canada indicate a salinity decrease from 30 g/L to 20 g/L and 26 g/L, respectively, within the uppermost 5 m of marine sediment. To investigate the mechanisms driving OFG formation in the region, we conducted three-dimensional numerical simulations of coupled variable-density groundwater flow and salt transport, incorporating detailed analyses of the region's topography, stratigraphy, and geological structures. Our findings indicate that sub-ice-sheet recharge and meteoric recharge are the primary processes responsible for OFG emplacement since the Last Glacial Maximum. The modeled OFG volume is 57,950 km^3, while the total submarine groundwater discharge across the entire Gulf is estimated at 1.15 km^3/year. Anisotropy in geological formations facilitates hydraulic connections between onshore and offshore aquifers, promoting active recharge of OFG. This onshore-offshore connectivity is reinforced by lower hydraulic conductivity, thicker unconsolidated marine sediments, greater anisotropy, and interlayered aquitards. Sensitivity analysis demonstrates that the system's behavior varies across the range of plausible geologic connectivity, transitioning from active flow dynamics in highly connected settings to a more passive regime in less connected configurations. This study highlights how geological and hydrological factors influence the distribution and availability of OFG resources in the region. Understanding the existence and function of the OFG system could inform the potential development of an alternative freshwater resource for the province of Prince Edward Island that is entirely groundwater reliant and faces competing water demands from domestic water users and the intensive agricultural industry.

1. Introduction

Groundwater is a crucial resource that sustains billions of people globally, playing an essential role in agriculture and supporting ecosystems (Gleeson et al., 2012; 2016). In Canada, despite the abundance of surface water, approximately 30 % of the population relies on groundwater; and this dependence is growing, particularly in the Atlantic provinces (Rivera and Nastev, 2005). Globally, humans are overexploiting groundwater in many large aquifers that are critical to agriculture, leading to groundwater depletion and associated land subsidence, especially in Asia and North America (Aeschbach-Hertig and Gleeson, 2012; Gleeson et al., 2012). As freshwater shortages worsen in major coastal cities, attention has turned to the potential exploitation of offshore freshened groundwater (OFG), a phenomenon observed worldwide (Micallef et al., 2021; Post et al., 2013). 'Freshened' refers to water in the sub-seafloor with a total dissolved solid concentration below that of seawater (Micallef et al., 2021). OFG has been discovered in both clastic and carbonate sedimentary deposits found on continental

* Corresponding author.
E-mail address: shengchao.yu@dal.ca (S. Yu).

https://doi.org/10.1016/j.jhydrol.2025.134553
Received 21 March 2025; Received in revised form 22 September 2025; Accepted 2 November 2025
Available online 7 November 2025

shelves, including those located in the Pacific Ocean (Faghih et al., 2024; Hesse and Harrison, 1981; Micallef et al., 2020; Morgan and Mountjoy, 2022), the Atlantic Ocean (Cohen et al., 2010; Thomas et al., 2019), the Indian Ocean (Morgan et al., 2018), the South China Sea (Kwong and Jiao, 2016; Sheng et al., 2023), the Gulf of Mexico (Person et al., 2017), and the Eastern Mediterranean (Paldor et al., 2020b). Understanding the mechanisms behind the formation and evolution of OFG systems, as well as the factors that control their distribution and connection to onshore aquifers, is critical to assessing whether these could offer a long-term solution to the growing water crises in coastal cities.

Possible mechanisms for the formation of OFG include (1) meteoric recharge, where groundwater is driven by topographic gradients during periods of sea-level lowstands (Edmunds and Milne, 2001; Sheng et al., 2024) or under current hydrologic conditions (Michael et al., 2016; Paldor et al., 2020b) and (2) sub-ice-sheet recharge, where groundwater flow is reorganized under large ice sheets, such as those that covered the continental shelves during the Last Glacial Maximum (LGM) (Person et al., 2003, 2007, 2012). The exposure of the continental shelf during lowstands to rain or ice melt is a critical factor facilitating fresh recharge and influencing groundwater movement. OFG systems can also be categorized into two types based on present-day conditions: active and passive (Paldor et al., 2024). Active OFG systems involve present-day onshore-offshore groundwater flow, often linked to offshore submarine groundwater discharge (SGD). In contrast, passive OFG reservoirs are remnants of ancient groundwater deposits that no longer have a hydraulic connection to onshore aquifers. Specific geologic conditions facilitate active OFG reservoirs, such as extensive interlayered aquitards at depth (Varma and Michael, 2012), heterogeneous aquifers that maintain onshore-offshore geological continuity (Michael et al., 2016), dynamic seepage processes along the continental slope (Hong et al., 2019), and subsea faults (Paldor et al., 2024). Passive OFG reservoirs are highly susceptible to saltwater intrusion during paleo-hydrological cycles, making it important to identify the hydrogeological characteristics of subsea aquifers and overlying aquitards that control seawater and groundwater interaction (Yu et al., 2023a).

Numerical models of different complexity have been used to investigate how hydrogeological controls influence OFG systems, including: 1) the origin and extent of fresh paleo-groundwaters on continental shelves (Cohen et al., 2010), 2) the role of present-day onshore recharge on OFG (De Biase et al., 2024), 3) the extent to which offshore freshwater supports onshore (Knight et al., 2018) and offshore (Yu et al., 2019) pumping, 4) the role of paleochannels and lava tubes in groundwater and seawater exchange (Kreyns et al., 2020; Mulligan et al., 2007), 5) the role of subsea aquifers with overlying aquitards in originating OFG (Solórzano-Rivas and Werner, 2018), and 6) the influence of geological heterogeneity of coastal sediments on OFG volumes (Zamrsky et al., 2020). However, these studies did not incorporate a three-dimensional analysis of topography, stratigraphy, and geological structure to fully evaluate the impact of hydrogeological characteristics. A 3D model analysis allows for the representation of lateral flow paths, complex shoreline geometries, and 3D spatial heterogeneity in aquifer properties, features that are especially important for understanding OFG dynamics. The development of a 3D model also enables a more accurate assessment of the volume and spatial distribution of OFG. These aspects cannot be fully captured in a 2D framework and are essential for gaining detailed insights into OFG evolution.

The continental shelf surrounding the Canadian province of Prince Edward Island (PEI) offers a unique hydrogeological setting. Unlike many offshore islands, PEI is geologically connected to the mainland, and the growth and collapse of the Laurentide Ice Sheet during Pleistocene glacial and interglacial cycles created extensive pathways of freshwater delivery (Marshall and Clarke, 1999). We hypothesize that ice sheet dynamics during the LGM facilitated the recharge of offshore aquifers through continental drainage pathways and that the freshened groundwater has been preserved despite subsequent sea-level rise (SLR), avoiding widespread downward saltwater intrusion due to the presence of unconsolidated marine sediments.

Given the lack of data on OFG in the Gulf of St. Lawrence (hereafter "Gulf"), numerical models provide valuable insights into how these systems developed, persist, and respond to varying hydrogeological conditions. In this study, a 3D geological model was first constructed based on borehole and geophysical data and then represented in a variable-density groundwater flow and solute transport model. The hydrogeological model was employed to specifically address three key objectives: (a) determine the primary processes responsible for OFG emplacement during paleo-hydrological cycles, (b) investigate how Quaternary marine sediments influence the hydraulic connection between seawater and offshore groundwater, and (c) understand the connection between onshore and offshore aquifers in response to varying hydrogeological conditions. This integrated modeling approach underscores the importance of understanding the interrelationships among oceanic, geologic, and hydrogeologic conditions that impact the dynamics of offshore groundwater systems, offering valuable insight for managing these critical resources under changing environmental conditions.

2. Materials and methods

2.1. Study area

The population of the Canadian Maritime Provinces is disproportionately reliant on groundwater, with PEI 100 % groundwater dependent for both drinking water and irrigation. PEI, Canada's most densely populated province, has an economy heavily tied to agriculture. However, groundwater on PEI faces growing quantity and quality challenges due to extensive agricultural practices and the effects of climate change on sea level and the hydrological cycle (Jiang et al., 2015; Oliver et al., 2024; Paradis et al., 2016, Pavlovskii et al., 2023).

Below PEI and the surrounding Gulf, the younger Carboniferous succession has been characterized through borehole and seismic data, identifying four distinct formations (Fig. 1b). These strata rest on the Port Hood Formation of the Cumberland Group in the east and extend westward over Mississippian rocks onto the basement (Gibling et al., 2019). At the base, the Bradelle Formation, dominated by sandstone with gray and red shales and interspersed coal and coaly shales, thickens toward Cape Breton Island (Fig. 1a). Above it, the Green Gables Formation is rich in shale and coal, while the overlying Cable Head and Naufrage formations primarily consist of sandstone, red shale, and pedogenic carbonate. These formations correspond to the upper strata of the Cumberland Basin in northern Nova Scotia (Gibling et al., 2019). The sandstone of Naufrage formation with fractures constitute the main aquifer in this area (Paradis et al., 2006, 2016). PEI lies within the Maritimes Basin, where abundant groundwater is available in Carboniferous formations, notably within the Pictou Group's Naufrage Formation sandstone aquifers (Paradis et al., 2016). Therefore, it is possible that fractured consolidated deposits in the Gulf also contain freshened waters, likely emplaced post-glacially during periods of subaerial exposure on the continental shelf (Shaw et al., 2002, 2006). In terrestrial environments, surficial unconsolidated deposits are typically unsaturated and not regarded as aquifers (Paradis et al., 2016). Marine sediments are present at some levels, but the connection to the open ocean is limited.

PEI and its adjacent continental shelf experienced a dramatic sea-level response produced by the last transition between glacial and interglacial climatic conditions, and the migration of paleo-coastlines altered the sedimentary environments at the surface boundaries (Fig. 1a). At the LGM, ice extended to the continental shelf's edge; by 15 ky BP (before present), the Gulf ice margin had moved to the St. Lawrence Estuary, and PEI was hydraulically connected to the Gulf. By 6 ky BP, the geography of the region was very close to the present one, with PEI and the Gulf separated (Shaw et al., 2002, 2006).

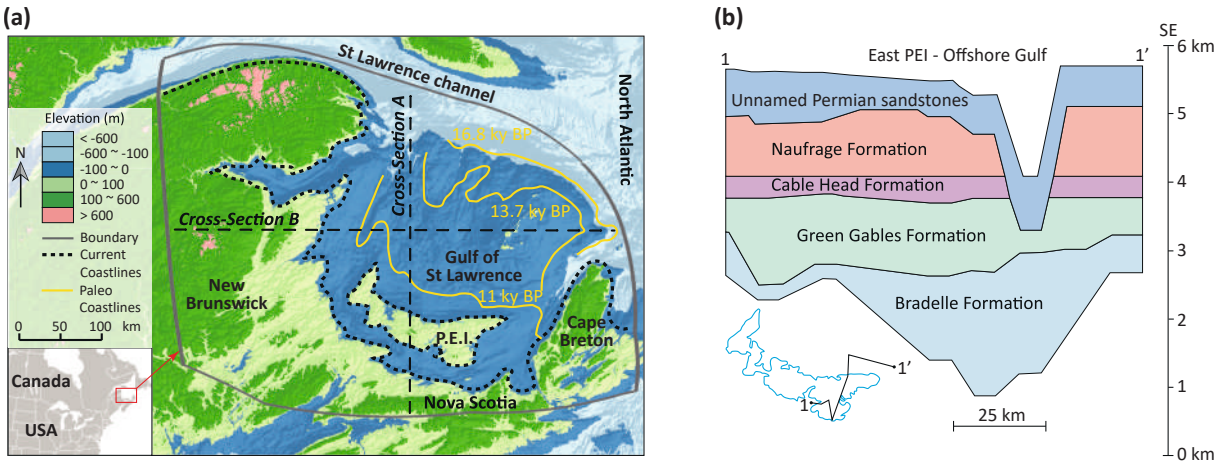

Fig. 1. Regional setting of PEI, the Gulf of St. Lawrence, and other eastern Canadian provinces: (a) topographic features of the Maritimes basin and changes of paleo-coastlines (Waelbroeck et al., 2002); (b) simplified cross-section through east PEI and part of the southern Gulf basin (Gibling et al., 2019).

2.2. Geological model

Borehole data were used to construct a geological model, as borehole information provides the most direct evidence of subsurface geology. Borehole data from the Maritimes Basin stratigraphy in PEI and the adjacent Gulf region were collated (Barss et al., 1979; Giles and Utting, 1999; Grant and Moir, 1992; Rehill, 1996). Most of the boreholes are located on land, with a smaller number situated offshore that were drilled for oil and gas exploration (Fig. 2a). Previous studies have yielded valuable stratigraphic insights from extensive seismic surveys in this area, focusing on geological and natural resource exploration (Atkinson et al., 2020). The geophysical data from this basin aligns with the geological layers revealed by borehole data. High-quality seismic lines were selected to derive stratigraphic information across various locations (Fig. 2a), and the drilled boreholes were used to calibrate geophysical data. In total, 124 boreholes were compiled (Fig. 2a), with approximately one-quarter classified as real boreholes. Ten distinct hydrogeological units were identified across stratigraphic formations when describing the core samples from each well (Fig. 2b). Finally, key borehole features, including the reference surface elevations as well as the top and bottom elevations of each hydrogeological unit, were documented and imported into ArcGIS to facilitate the construction of a

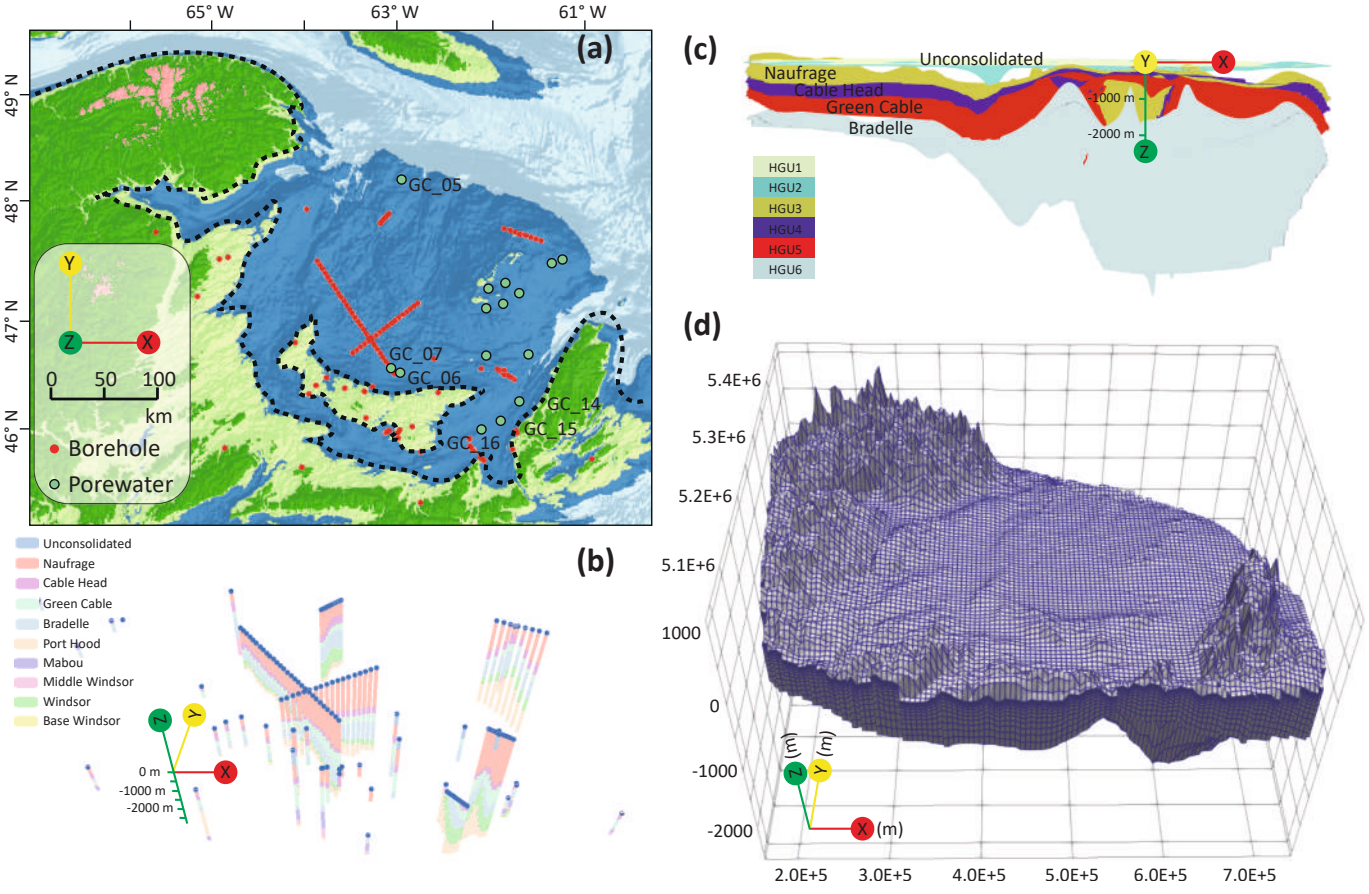

Fig. 2. (a) Borehole locations, (b) *Borelines* used in ArcGIS, (c) geological layers, and (d) model grid in HydroGeoSphere.

detailed geological model.

Arc Hydro Groundwater (Strassberg et al., 2011), a data model developed for use within the ArcGIS environment, involves three primary steps: framework, subsurface, and simulation. In this study, the first two steps were applied to generate a geological model through the classification and visualization of borehole logs. Initially, *Borelines* were created for each well based on hydrogeologic units across different locations. The next step involved generating *BorePoints* from the borehole data. Finally, geological layers representing stratigraphic horizons were constructed within the 3D model. These geological layers were interpolated by connecting *BorePoints* with matching attributes across different formations. This approach provides a clear visualization of the 3D geological structure of the Maritimes Basin stratigraphy in PEI and surrounding Gulf region. Stratigraphic files for the geological layers were imported into the numerical groundwater model for vertical discretization. In this way, the hydrogeological zones in each layer used for groundwater model parameterization were delineated based on the 3D geological model. Aquifer hydraulic parameters, including hydraulic conductivity, anisotropy, and specific storage, were later assigned to each hydrogeological zone.

2.3. Hydrogeological model

The groundwater flow and solute transport simulations were conducted using HydroGeoSphere, a three-dimensional model that integrates subsurface and surface flow through control volume finite elements, utilizing parallel processing and adaptive time-stepping (Aquanty, 2022). Due to the difficulty in determining surface flow channels post-LGM, the surface flow module was not activated in this model. HydroGeoSphere has been widely applied to coastal groundwater studies, effectively accounting for factors such as sea-level rise, tidal fluctuations (LeRoux et al., 2023; Yang et al., 2015), and storm surges (Guimond and Michael, 2020; Paldor and Michael, 2021; Yu et al., 2016). The model simulates variable-density effects on groundwater flow using an equivalent freshwater head approach (Frind, 1982). Full governing equations for flow and transport, along with details on the surface–subsurface coupling methods, are provided by Aquanty (2022).

The numerical model was developed based on the comprehensive geological reconstruction and spans a rectangular area of 580 × 450 km^2, divided into 2,500 m × 2,500 m grid cells for horizontal discretization (Fig. 2d). The spatial extent of the geological and numerical model, which extended to the natural groundwater divides outside of the Gulf, was determined through a numerical model sensitivity analysis of the impact of different boundary locations on the flow field in the aquifer of interest as detailed in the Supplementary Material S1. The coordinate reference system NAD83 / UTM zone 20 N is used as it is particularly suited for areas in eastern Canada. The surface elevation is based on a simplified provincial digital elevation model (Natural Resources and Renewables, 2006) (Fig. 1a), while the model base extends between 600 and 2400 m below sea level (Giles and Utting, 1999). Vertical discretization was achieved through 25 horizontal layers of increasing thickness with depth, designed to capture subsurface stratification effectively. Geological layering was incorporated by importing GIS-based stratification data into HydroGeoSphere. This approach yielded a model domain with 221,442 nodes and 207,800 elements, totaling a volume of 195,028 km^3 that spans from the Maritimes Basin to the Gulf (Fig. 2d). Given the model size, complex non-linear equations, long-term simulation period, and stringent convergence requirements, simulations were run on multiple cores of the Cedars high-performance computing cluster, supported by the Digital Research Alliance of Canada (see acknowledgments).

Boundary conditions were established for both recharge and subsurface domain boundaries. A constant recharge rate of 521 mm/year, drawn from previous hydrogeological studies on PEI (Jiang et al., 2004; Jiang & Somers, 2009; Stanic et al., 2024), was applied as a representative value to the land surface above the real-time sea-level. At the seaward boundary along the top of the model, sea-level changes over the past 20,000 years, from −120 m relative sea-level (RSL) to present levels, were specified (Waelbroeck et al., 2002). A sea-level reconstruction along the PEI coastline (Vacchi et al., 2018) was also incorporated as the seaward boundary in a sensitivity scenario to evaluate the influence of different regional boundary conditions. To account for the shifting shoreline due to sea-level change, the seawater concentration boundary and specified-head boundary were extended landward throughout each hydrologic interval (Cantelon and Kurylyk, 2024; Yu et al., 2023b). Present-day bathymetric data (GEBCO, 2022) were used to determine the offshore position of the coastline during periods of lower sea-level. For saltwater intrusion, a seawater concentration (C/Co = 1) was assigned to any incoming saltwater flows, while the model computed concentrations for outgoing flows based on local saltwater-freshwater balances in each cell. Groundwater salinity < 1 g/L (i.e., C/Co = 0.02857) is defined as OFG in this study. The variable-density effect was simulated by assigning a freshwater concentration of 0 g/L with a density of 1,000 kg/m^3 and a seawater concentration of 35 g/L with a density of 1,025 kg/m^3 (Waelbroeck et al., 2002). No-flow and no-solute transport conditions were applied at the bottom, vertical landward, and vertical seaside boundaries. A sensitivity test on the seaside boundary indicated that when the side boundary to the open sea was changed from closed to open, the impact on the numerical simulation results was nearly negligible. The steady-state groundwater head and salinity distribution at −120 m RSL during 20 ky BP were used as initial conditions for the transient simulation.

In the hydrogeological model, unconsolidated marine sediments and the Naufrage formation layers were represented as the top aquitard and the lower aquifer, respectively. The aquifer system comprised a shallow, high-flow zone and a deeper, low-flow zone (Savard et al., 2007). The shallow zone exhibited high hydraulic conductivity (K) but limited specific storage (S_s), with K values generally decreasing with depth. To reflect these variations, the Naufrage formation aquifer was subdivided into nine layers, each with distinct hydrogeological parameters. Subsurface properties were informed by prior studies (Paradis et al., 2016), field investigations (Savard et al., 2007), and model defaults (Table 1). Vertical hydraulic conductivity (K_z) and storage values were selected based on field data (Paradis et al., 2016; Savard et al., 2007) and model calibration. Anisotropy ratios in the model layers (Table 1) were derived from a hydrogeology study on PEI's fractured sandstone (Savard et al., 2007) and applied as typical values in this modeling study. Due to mesh size constraints and the Peclet number, dispersivity was set to a longitudinal (α_L) value of 10.0 m, with both transverse (α_T) and vertical (α_V) transverse dispersivities set at 10 % of this value (Voss and Souza, 1987).

Results from the marine research survey Cruise No. MSM103 carried out in the Gulf in 2021 yielded porewater data from gravity cores of the shallow sediment (Schulten et al., 2022). Despite being depth-limited, these porewater salinity profiles can be used for the calibration of the

Table 1
Base-case model parameters and their values used in simulations. (a. Paradis et al., 2016; b. Savard et al., 2007; c. Voss and Souza, 1987).

Characteristic	Layer	K_x (m/s) [a, b]	S_s (1/m) [a, b]	Anisotropy (K_x: K_z) [b]	Dispersity (m) α_L: α_T: α_V [c]
Aquitard	Marine sediment	1E-7	7E-5	10	10, 1, 1
Aquifer	Naufrage_1	1E-4	1E-6	2	10, 1, 1
	Naufrage_2	1E-5	1E-5	5	10, 1, 1
	Naufrage_3	5E-6	2E-5	10	10, 1, 1
	Naufrage_4	4E-6	3E-5	10	10, 1, 1
	Naufrage_5	3E-6	4E-5	10	10, 1, 1
	Naufrage_6	2E-6	5E-5	10	10, 1, 1
	Naufrage_7	1E-6	6E-5	10	10, 1, 1
	Naufrage_8	1E-7	7E-5	1	10, 1, 1
	Naufrage_9	1E-8	8E-5	1	10, 1, 1

3D hydrogeological model. The main calibration parameters were hydraulic conductivity values in the aquifers and unconsolidated marine sediments. Gravity coring was accomplished in various working areas in the Gulf offshore PEI during the Cruise No. MSM103, and six successful coring boreholes were selected for the present study, with five cores collected within 30 km off the coast of PEI and another one around the St. Lawrence Estuary (Fig. 2a). Gravity coring was conducted at seawater depths ranging from 46 to 121 m, with selected core lengths ranging from 2.80 to 4.62 m. Hydraulic parameters could be better constrained through additional borehole hydraulic testing and geophysical surveys that provide spatial salinity distributions. The latter will be explored in future work for the SOURCE project (Maselli, 2022).

2.4. Controls on OFG dynamics

A base-case model (Run 1) was developed using the parameters listed in Table 1 and used to analyze key processes that govern the Gulf OFG dynamics through the transient simulation. As summarized in Table 2, a sequence of model runs was undertaken to (1) investigate the hydraulic connection between seawater and offshore groundwater impacted by the hydraulic conductivity, anisotropy, and thickness of unconsolidated marine sediments, and (2) assess horizontal and vertical groundwater flow within offshore aquifers accounting for the anisotropy of aquifers and the presence of interlayered aquitards within the main aquifer system.

Sensitivity studies (Table 2) considered the anisotropy of aquifers and aquitards (Runs 2–4), variations in K (Runs 5–6) and thickness (Runs 7–8) of unconsolidated marine sediments, and the presence of interlayered aquitards within the main aquifer system (Runs 9–10). The anisotropy ratio of each layer was multiplied or divided by 2 (Runs 3–4, Table 2), and a scenario with a high anisotropy ratio of 100 (Run 2) was run, for which the K_x was maintained while the K_z changed. These simulations test the sensitivity of the system behavior to the upscaled effect of horizontally oriented aquifer heterogeneities. Anisotropy ratios are difficult to estimate with sparse data but have been shown to be substantially higher than 100 in large, heterogeneous basins (e.g., Keating et al., 2005; Michael and Voss, 2009a, 2009b; Williamson et al., 1990). The K range of unconsolidated marine sediments ($1 \times 10^{-4} \sim 1 \times 10^{-8}$ m/s) was decided based on in-situ measurement of consolidation and permeability of soft marine sediments (Christian, 1993), and empirical values for the thickness of marine sediment (0.4–4 % Naufrage formation) were derived from studies on sediment distribution in the Atlantic Ocean (Ewing et al., 1973) and sediment thickness in the western North Atlantic (Giles and Utting, 1999; Tucholke et al., 1982). High K of marine sediments indicates that they are coarse grained. The distribution of interlayered aquitards in subsea aquifers is a common phenomenon (Solórzano-Rivas and Werner, 2018; Sheng et al., 2024); accordingly, the layers of Naufrage_4 and Naufrage_6 were replaced by a hypothetical aquitard of the same K as the marine sediments (Runs 9–10) to explore the potential effects of aquitard distribution at various levels within the main offshore aquifer system.

Table 2
Multiple scenarios for sensitivity analysis: varying properties of unconsolidated marine sediments (Runs 1–5), varying anisotropy (Runs 6–8), and incorporating layered aquitards within the primary aquifer system (Runs 9–10). The marine sediment thickness is expressed as a % of aquifer thickness. Typical anisotropy values are given in Table 1.

Run ID	K_x (m/s)	Sediment thickness	Anisotropy	Layered aquitard
Run 1	1E-07	1 %, 2.8~7.5 m	layered typical values	No
Run 2	1E-07	1 %, 2.8~7.5 m	**100**	No
Run 3	1E-07	1 %, 2.8~7.5 m	**layered typical values × 2**	No
Run 4	1E-07	1 %, 2.8~7.5 m	**layered typical values/2**	No
Run 5	**1E-04**	1 %, 2.8~7.5 m	layered typical values	No
Run 6	**1E-08**	1 %, 2.8~7.5 m	layered typical values	No
Run 7	1E-07	**0.4 %, 1.1~3.0 m**	layered typical values	No
Run 8	1E-07	**4 %, 11.2~30.0 m**	layered typical values	No
Run 9	1E-07	1 %, 2.8~7.5 m	layered typical values	**aquitard layer_4**
Run 10	1E-07	1 %, 2.8~7.5 m	layered typical values	**aquitard layer_6**

3. Results

3.1. Geological model

The 3D geological model developed through integrating available borehole logs, geophysical information, and other information (Atkinson et al., 2020; Barss et al., 1979; Giles and Utting, 1999; Grant and Moir, 1992; Rehill, 1996) is available as digital products in the electronic supplementary material S1. The 3D model (Fig. 2c) shows that the bounding surfaces are continuous across the model domain, with no major faults identified in this margin setting. The sequences form a seaward thickening wedge, with the maximum dip-direction toward the northeast. The sea floor topography is relatively flat in the Gulf region. The geological model in Fig. 2c shows five model layers with the layer thickness varying from 20 to 2000 m, summing to a total thickness of 5000 m.

3.2. Model calibration

The high-level salinity calibration in Fig. 3 shows that the model reproduced the salinity trends observed in sediment cores resulting either from freshening in the shallow aquifer or direct vertical saltwater intrusion. Notably, boreholes monitoring freshwater were located in areas between adjacent salt fingers, consistent with the freshwater zones simulated in the model (see Section 3.3 for further discussion). The observed deviations in model calibration, such as at GC_15, can likely be attributed to the highly heterogeneous distribution and variable thickness of Quaternary marine sediments in the Gulf, as documented in previous investigations (Josenhans and Zevenhuizen, 1993).

3.3. Sea-level rise simulations

The numerical model was run from the LGM to the present to investigate the impacts of past sea-level change on the development and evolution of the OFG system. The transient simulation Run 1 indicates the freshwater/saltwater interface movement under paleo precipitation and rising sea level over the past 20 ky. Fig. 4 shows the simulated salinity distributions since the LGM. To illustrate the distribution of groundwater salinity, two cross-sections were selected: one traversing PEI from south to north and one west to east from NB inland to the Gulf (Fig. 1a). At around 14 ky BP, seawater began to intrude into the northeast boundary of the model domain (Fig. 4a1). At this time, inland freshwater flowed through the entire aquifer system at a relatively high velocity (up to 25 m/year), driven by the steep hydraulic gradient between the inland basin and the shoreline (0.8–2.2 ‰). Fig. 4b1, c1 show that a large, freshened groundwater body was stored in aquifers after the LGM, extending almost to the edge of the continental shelf. The freshwater/saltwater interface is predicted to occur at $x = 705$ km in cross-section B, which is 350 km away from the current coastline.

During the early Holocene (Fig. 4a2, a3) from 12 ky BP to 10 ky BP, seawater inundated low-lying areas, and saltwater intrusion first appeared in the shallow Naufrage formation as salt fingers (Fig. 4b2, c2, b3, c3). Freshwater from the deep aquifer seeps upwards into the shallow aquifer, causing complex upwelling and mixing processes due to buoyancy effects. Thus, although there is a moderate surface area of seawater inundation (Fig. 4a3), the saltwater intrusion in the subsurface is manifested only in thin saltwater bodies (Fig. 4b3, c3). At this stage,

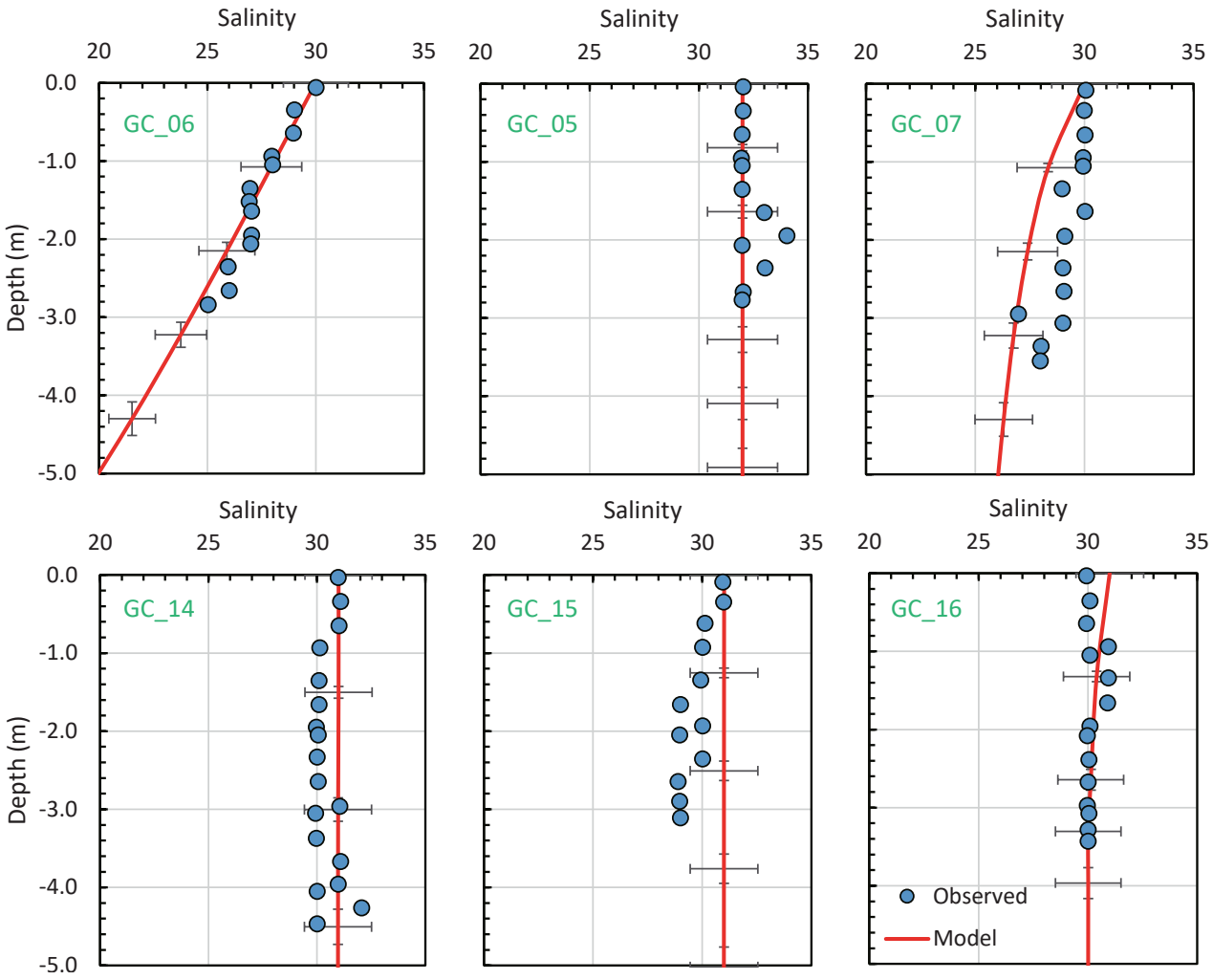

Fig. 3. Modeled versus observed groundwater salinity profiles in the Maritimes basin and adjacent continental shelf. The red lines represent the simulated profiles for Run 1. The locations of gravity cores with porewater information can be found in Fig. 2a. (For interpretation of the references to colour in this figure legend, the reader is referred to the web version of this article.)

approximately half of the Gulf was submerged, and the strong hydraulic connection between the inland and offshore systems extended beyond the coastline, reaching up to 100 km offshore.

Over the following four millennia, although the sea-level rise rate was only one-third of that of the early Holocene period (Waelbroeck et al., 2002), the saltwater plume advanced deeper into the aquifer (Fig. 4b4, c4, b5, c5). It is worth noting that at 6 ky BP, when the sea level rose to almost the same level as it is today (Fig. 4a5), there was still a large volume of OFG under the seabed as shown in cross-section A at y = 5170~5370 km and cross-section B at x = 400~650 km (Fig. 4b5, c5).

In the last 6 ky, sea-level changes have not been significant, but due to recharge limitations and solute dispersion, salt fingers gradually developed laterally and vertically (Fig. 4b6, c6), reducing the OFG volume. However, the development of salt fingers was constrained by the horizontal flow, enabled by the hydraulic connection between onshore and offshore aquifers. Most of the OFG placed at cross-sections A & B in the last stage has been preserved (Fig. 4b6, c6). At present sea level, the model indicates inland fresh groundwater can be discharged to nearly 50 km offshore to the north of PEI and more than 50 km offshore to the east of Nova Scotia. Conversely, no hydraulic connection between onshore and offshore aquifers is found east of New Brunswick (Fig. 4a6). This model run suggests that the OFG is actively recharged from PEI and eastern Nova Scotia aquifers.

These results are based on the model with the sea-level reconstruction for the Atlantic coast (Milliman and Emery, 1968; Waelbroeck et al., 2002) applied as a dynamic specified head boundary condition. However, a different simulation used the sea-level reconstruction for the southern Gulf (Vacchi et al., 2018), which introduced more saltwater intrusion into offshore aquifers (Fig. S3). Also, the onshore-offshore connection was affected near the north of PEI but still present. We focus our results on the simulations with the regional boundary based on the sea-level reconstruction for the Atlantic coast because whether the reconstructed sea-level change based on collected samples very close to PEI can be extended to the entire Gulf is worthy of careful consideration, and the regional 3D model is not limited to PEI, but also includes Nova Scotia, New Brunswick and even the St. Lawrence channel. Using the sea-level reconstruction for the southern Gulf may cause some errors in other areas in the regional model.

3.4. Sensitivity analysis

Given the uncertainties in unconsolidated marine sediment permeability, thickness, and anisotropy as well as the presence of interlayered confining units within the main aquifer system, we conducted a sensitivity study to understand how these factors influence the distribution of freshened groundwater resources in an idealized continental-shelf aquifer system based on transient simulations.

Simulations 2–4 tested the effects of aquitard and aquifer anisotropy by varying K_z relative to K_x. Higher anisotropy values (Run 3) reduced

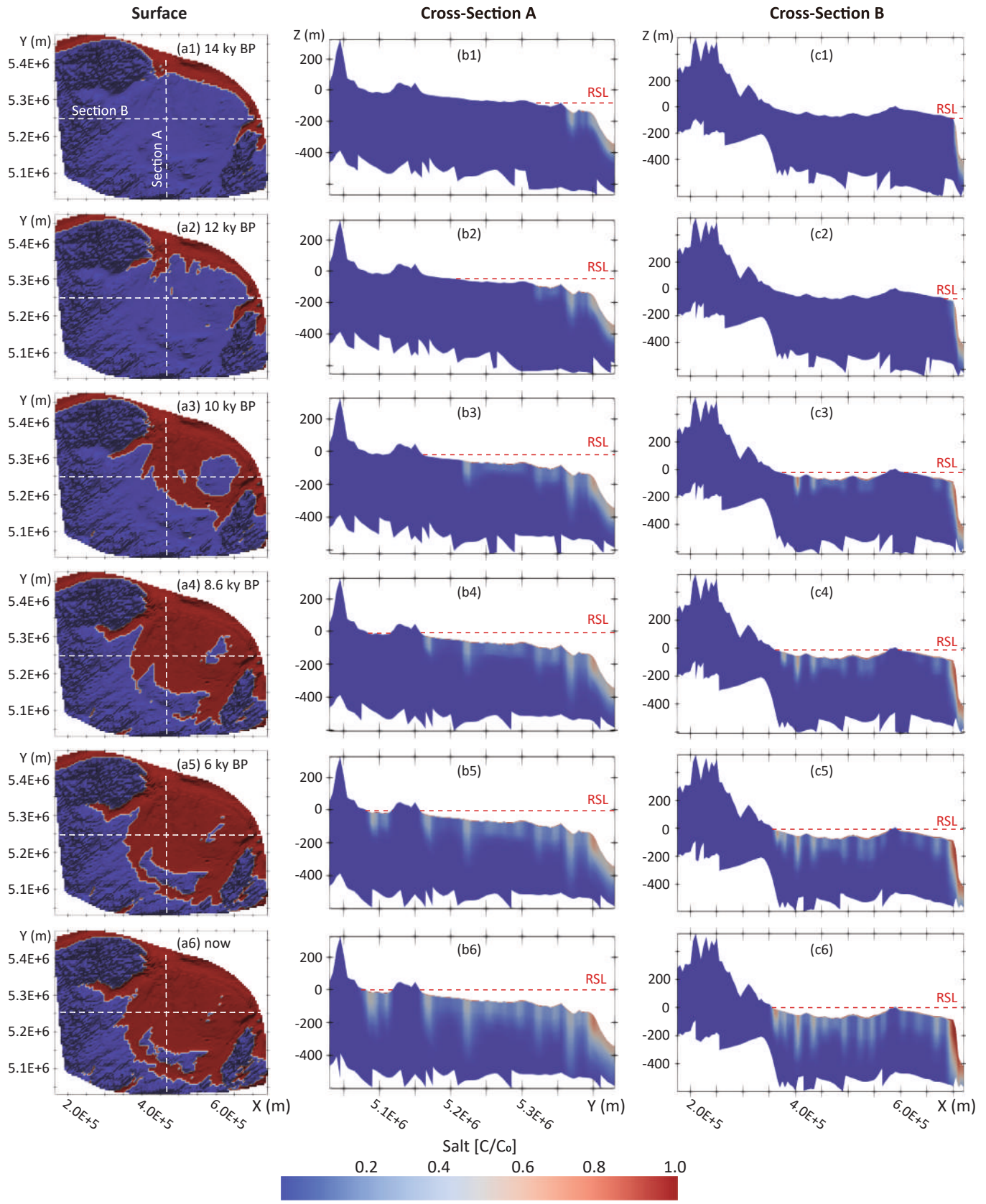

Fig. 4. Distributions of surface water salinity in top view (a) and groundwater salinity at cross-section A (b) and B (c) for the transient simulations at times: 14 ky BP, 12 ky BP, 10 ky BP, 8.6 ky BP, 6 ky BP and now. The locations of cross-sections can be found in Fig. 1a. To clearly express the growth of the vertical finger, the aquifer below $z = -600$ m was cut away; below $z = -600$ m it is full of fresh groundwater. The full view of the model domain is shown in supplementary material S1.

saltwater infiltration, resulting in more OFG (59,840 km^3) and shorter salt fingers (Fig. 5a3, b3). Reducing anisotropy (Run 4) prevented the preservation of OFG, allowing salt fingers to develop downward (Fig. 5a4, b4). When a constant anisotropy value (e.g., 100 for Run 2) was applied across the hydrogeological system, salt fingers were absent, and salt plumes were confined to surficial marine sediments (Fig. 5a2, b2). Flowline patterns (Fig. S4) revealed that SGD from PEI and eastern Nova Scotia extends more than 50 km offshore, with the flow paths continuing to recharge OFG (62,323 km^3).

Two simulations were run with a single set of aquifer K while varying the K of unconsolidated marine sediment (10^{-4} m/s and 10^{-8} m/s). When marine sediment K increased (Run 5), saltwater intrusion intensified both in cross-sections A & B, and the OFG volume decreased (Fig. 5a5, b5). Higher marine sediment K facilitated vertical saltwater infiltration, reducing the OFG volume in Run 5 (51,325 km^3) to 88 % of that in Run 1 (57,950 km^3). The high marine sediment K scenario represents conditions for which marine sediments are thin and coarse-grained. However, under this no-mud-layer condition, the expected salinity decline in the shallow borehole was not observed, nor was there evidence of active onshore-to-offshore groundwater recharge. Conversely, reducing marine sediment K (Run 6) restricted saltwater intrusion in both cross-sections, with lower K effectively attenuating the impact of long-term seawater flooding (Fig. 5a6, b6). The reduction in saltwater intrusion allowed for the preservation of fresh groundwater (59,262 km^3) up to 1.02 times that in Run 1.

Simulations varying marine sediment thickness showed that thinner aquitards (0.4 % of aquifer thickness, Run 7) increased saltwater intrusion, particularly at $y = 5160{\sim}5180$ km and $y = 5220{\sim}5380$ km in cross-section A (Fig. 5a7). This change of marine sediment thickness reduced OFG volume by 3.8 % (2,202 km^3) compared to Run 1. Thicker aquitards (4 %, Run 8) facilitated greater inland freshwater flow into the subsea aquifer (Fig. 5a8, b8), preserving a substantial volume of OFG (62,784 km^3) in the Naufrage formation from the LGM to the present day.

Finally, simulations 9 and 10 introduced interlayered aquitards within the main offshore aquifer. Replacing the Naufrage_4 layer (Run 9) with a hypothetical aquitard limited deep saltwater intrusion ($z = -200 \sim -400$ m), preserving OFG volume (60,795 km^3) in the subsea aquifer (Fig. 5a9, b9). In contrast, replacing the deeper Naufrage_6 layer (Run 10) with a hypothetical aquitard provided less protection, as solutes intruded down to $z = -500$ m before being constrained (Fig. 5a10, b10). This result highlights the importance of shallow thin confining units between the various aquifer layers for the preservation of deep-sea OFG.

4. Discussion

4.1. Emplacement and development of OFG

The model results provide insight into the development mechanisms of OFG on the continental shelf surrounding PEI, as illustrated in Fig. 6. Around 21 ky BP, during the LGM, glacial ice extended to the edge of the continental shelf; then by 20 ky BP, the ice began to unground forming an ice shelf (Shaw et al., 2006). Subglacial melting, drainage networks, and the potential formation of proglacial lakes enabled significant sub-ice-sheet recharge across the continental shelf (Person et al., 2007), reorganizing subsurface flow systems (Fig. 6a). Groundwater recharge from adjacent provinces also contributed to a strong flow towards the estuary, setting the stage for OFG preservation beneath the current Gulf. By 18 ky BP, the continued delivery of ice to the ocean led to inland reductions in ice elevations, a process that spanned thousands of years (Shaw et al., 2006). During this time, meteoric recharge played an increasingly prominent role, especially with sea level at historic lows. The elevated hydraulic heads and steeper gradients, combined with localized vertical recharge through exposed continental shelves, further enhanced freshwater flow into the subsurface (Fig. 6b, 6e).

As sea level rose rapidly following the retreat of ice from the Gulf, the previously stored freshwater in the continental shelf became vulnerable to Holocene marine transgression. Anisotropy in geological formations plays a critical role by promoting predominantly horizontal groundwater flow (Anderson, 1989). This limits downward saltwater intrusion and increases the likelihood of SGD extending into offshore regions.

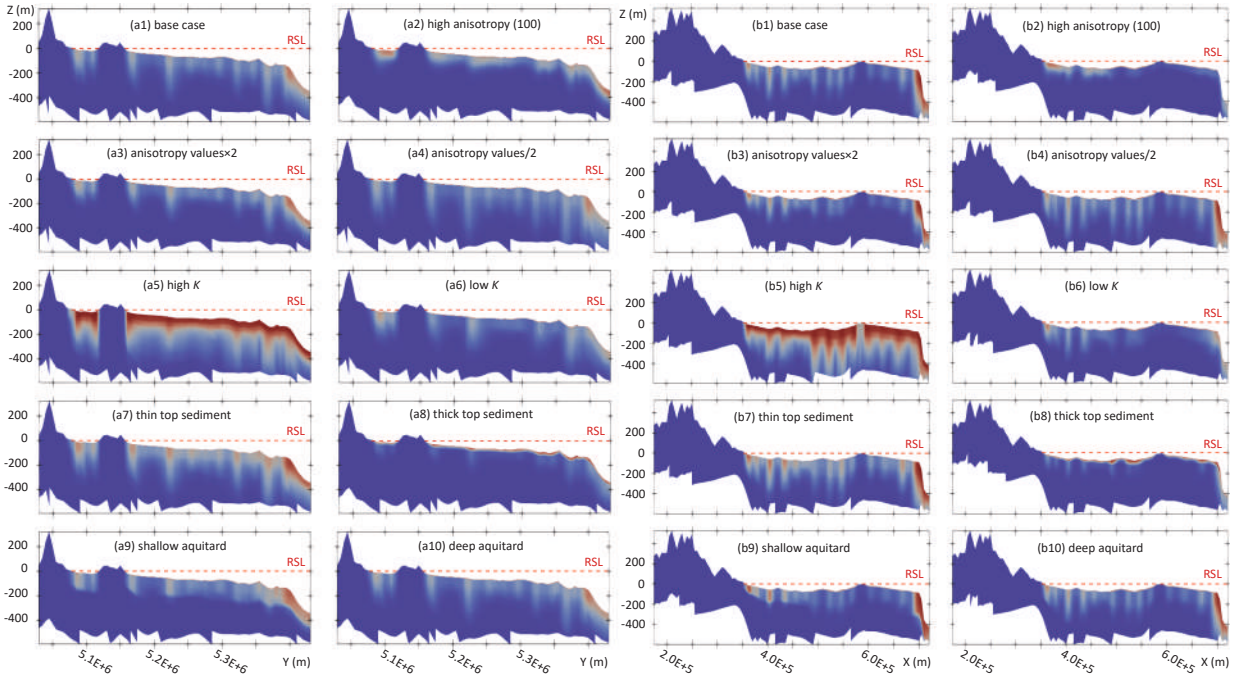

Fig. 5. Present-day distributions of groundwater salinity after transient simulations for sensitivity analysis at cross-sections A (a) and B (b), with the locations of cross-sections shown in Fig. 1a. To clearly express the growth of the vertical finger, the aquifer below $z = -600$ m was cut away; below $z = -600$ m it is full of fresh groundwater. The full view of the model domain is shown in supplementary material S1.

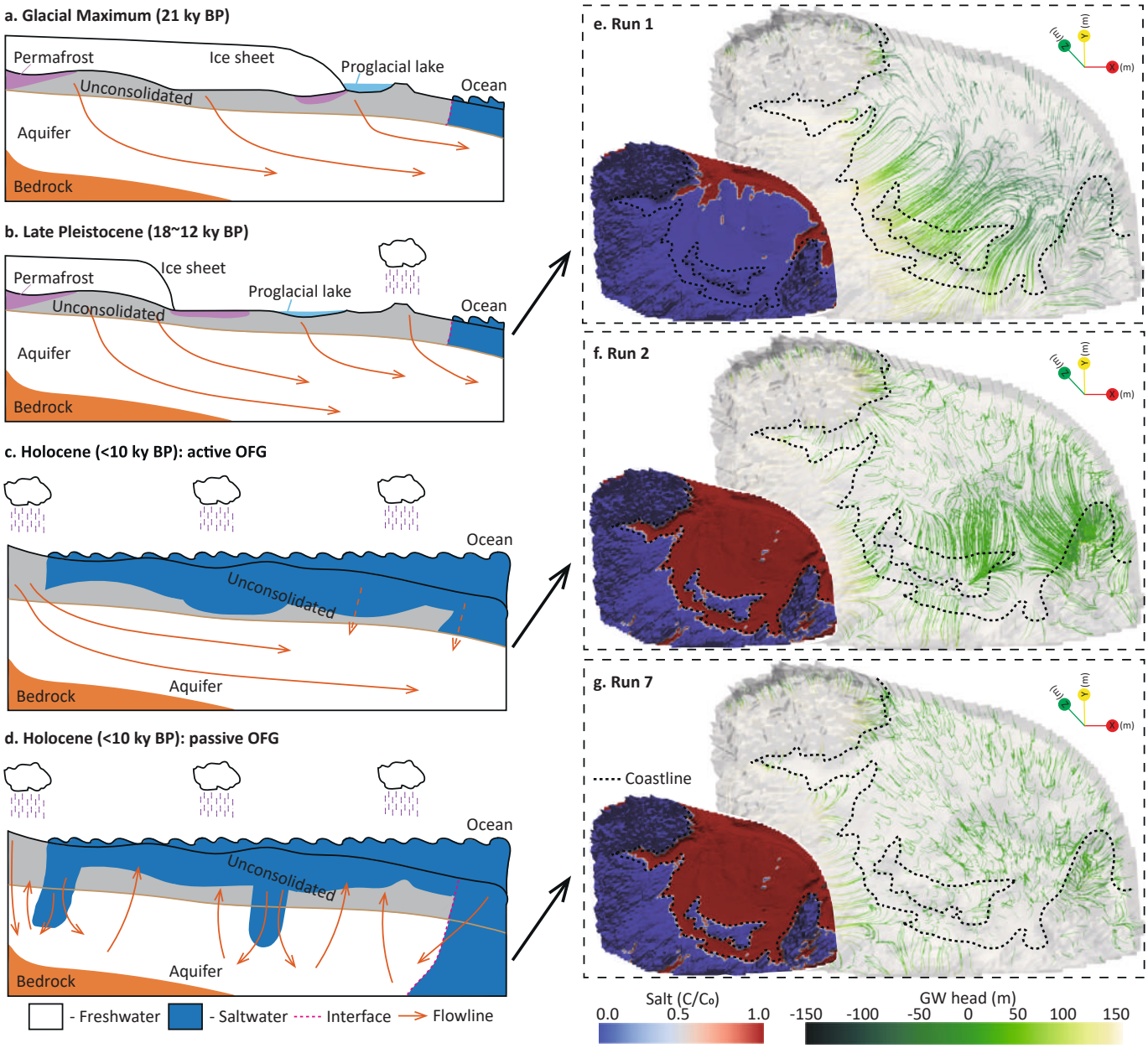

Fig. 6. Conceptual model of changes in groundwater across continental shelf surrounding PEI: (a) during the Laurentide Ice Sheet, (b) during late Pleistocene sea-level lowstands, and different scenarios of (c) active OFG, and (d) passive OFG. (e), (f), (g) denote 3D groundwater flow patterns of Runs 1, 2, and 7 corresponding to the time periods shown in (b), (c), and (d), respectively.

Simulations such as Run 2 reveal active recharge pathways for OFG through permeable connections between onshore and offshore aquifers. Geological anisotropy prevents fresh groundwater from discharging at the coastline, instead directing offshore flow and concentrating SGD further from the shore (Fig. 6c). Variations in coastline morphology along the shore lead to substantial spatial variability in lateral groundwater flow (Fig. 6f). In the eastern portion of PEI, SGD can extend hundreds of kilometers offshore, whereas in the western region, due to distinct topographic features and the proximity to NB, SGD is far less pronounced. Similarly, in Cape Breton, located at the easternmost tip of NS, SGD extends hundreds of kilometers offshore, while along the NB coastline, it is limited to only 10–20 km. These spatial contrasts underscore the benefits of a 3D modeling approach. The 3D simulations presented here reveal critical insights that cannot be captured by simplified 2D cross-shore models, specifically, the influence of geographically distributed inland groundwater sources on OFG across the entire Gulf-scale domain.

In scenarios with limited protection from unconsolidated marine sediments (Runs 5 and 7) or horizontal flow (Run 4), seawater began intruding into the aquifer in the form of salt fingers (Fig. 6d). The buoyancy of OFG was insufficient to counteract the weight of infiltrating saltwater, rendering the stored freshwater passive, without active recharge from onshore aquifers. Consequently, the preservation and distribution of OFG depended heavily on antecedent conditions. These isolated freshwater zones, disrupted by salt finger infiltration, are challenging to develop due to their discontinuous nature. The 3D model results demonstrate that localized circulation induced by salt fingering does not develop uniformly along a single cross-shore profile but is instead heterogeneously distributed across the entire Gulf (Fig. 6g). This spatial variability is challenging to capture using 2D models.

Fingering occurs in almost all cases except for the highly anisotropic scenario (Run 2). In this case, the inland fresh groundwater actively

flows offshore and discharges efficiently, preventing the formation of salt fingers (Figs. 6c, S4b). In other cases, salt fingering is observed, though the fingers do not extend deeply due to the protective influence of unconsolidated marine sediments and the presence of horizontal flow (Fig. 6d). Flowline analysis (Fig. S4a) indicates that some freshwater discharge limits the downward migration of salt fingers; however, the fresh groundwater discharge remains relatively weak, suggesting that salt fingers may continue to descend gradually. Over time, a dynamic competition between freshwater discharge and saltwater intrusion is expected to determine whether the system evolves into an active or passive regime.

Previous studies on the Atlantic Continental Shelf, such as Person et al. (2003), identified aquifer salinity less than 5 ppt more than 150 km offshore of Long Island, New York, and evaluated mechanisms like meteoric and subglacial recharge. Similarly, Cohen et al. (2010), reported fresh to brackish water, albeit nonrenewable resource, in shallow Miocene sands more than 100 km offshore of New Jersey. Our conceptual model for the continental shelf around the Atlantic provinces reveals similar mechanisms but also highlights the potential for both active and passive OFG.

4.2. Influence of geological and hydrogeological factors

Low-K unconsolidated marine sediments can limit saltwater intrusion into the subsurface. However, once saltwater breaches the surficial confining units, it forms salt fingers that can penetrate deeper aquifers, disrupting the recharge of OFG from inland sources (Fig. 5a5, b5). A study on continental-shelf freshwater resources in the passive-margin Atlantic Shelf of New England also showed that a reduction in confining-unit permeability decreases the amount of vertical leakage of saline water (Person et al., 2017). This effect is particularly noticeable when compared to the high anisotropy scenario, for which K_x remains unchanged but K_z is reduced (Fig. 5a2). In Run 2, salt plumes are primarily confined to shallow marine sediments and rarely migrate into deeper aquifers. The relatively enhanced horizontal flow in lower aquifers prevents vertical saltwater movement while promoting SGD further offshore. Although the geological settings differ, hydrogeological modeling of the eastern margin of the Maltese Islands demonstrates the broader conceptual relevance of anisotropy: a decrease in anisotropy leads to an overall increase in offshore groundwater salinity and a reduction in its offshore extent (Haroon et al., 2021).

The thickness of unconsolidated marine sediments has a clear impact on OFG distribution (Fig. 5a7, b7, a8, b8). The thin marine sediments introduce more obvious salt fingers which are about to cut off the onshore-offshore aquifer connection, while thicker marine sediments not only prevent most saltwater intrusion into lower aquifers but also promote SGD further offshore. This has also been confirmed in previous OFG studies. For example, a Pleistocene hydrogeology study of the Atlantic continental shelf, off New England revealed that the leakage is inhibited farther offshore by the increasing thickness of the overlying low permeability unit (Person et al., 2003).

The presence of an upper interlayered aquitard influences OFG distributions by mitigating vertical saltwater intrusion near the transition zone between seawater and the aquifer (Fig. 5a9, b9). This layer serves as a critical barrier, particularly in regions most vulnerable to saltwater intrusion. In contrast, middle interlayered aquitards exert a minor effect on vertical saltwater migration (Fig. 5a10, b10). These findings suggest that the upper confining units close to surficial marine sediments play a more pivotal role in protecting OFG resources from saltwater intrusion. While the geological context differs, geophysical surveys for the eastern margin of the Maltese Islands offer a conceptually relevant example: the absence of a confining unit above the resistivity anomalies was interpreted as evidence against extensive OFG, with localized pore fluid freshening instead occurring within permeable limestone layers bounded by confining units (Haroon et al., 2021).

4.3. Implications and limitations

Based on simulation results, we propose two potential mechanisms for the development and persistence of OFG in the continental shelf surrounding PEI. The 3D groundwater flow and solute transport model highlights the critical role of geological and hydrological parameters in regulating these mechanisms. This suggests that the geological and hydrological characteristics of sediments and aquifers significantly influence the distribution and availability of OFG resources in the region. Supporting this, the 2021 cruise investigation No. MSM103 for the SOURCE project reported a decrease in groundwater salinity with depth in gravity cores, along with high resistivity values corresponding to lower salinity levels (Schulten et al., 2022). This indicates the presence of freshened groundwater in the upper section of the seafloor. However, these observations were only made at shallow locations, and further analysis, including from marine controlled-source electromagnetic surveys, is underway to delineate the distribution of deeper groundwater salinity. While it remains difficult to define the specific volume and function of the OFG system in the Gulf based on the current model, this work contributes to broader efforts aimed at understanding the connections between onshore and offshore groundwater systems and the controls on OFG distribution. Our paleo-hydrogeological model integrates a 3D analysis of topography, stratigraphy, and geological structure to evaluate the impact of hydrogeological characteristics on OFG. Variations in cross-shore groundwater flow profiles across different locations off PEI underscore the spatial complexity of offshore hydrogeological systems, revealing that simplified 2D models are often inadequate to capture the alongshore heterogeneity, 3D flow pathways, and geological variability necessary for accurate characterization and prediction. However, it does not account for factors such as permafrost evolution and surface water drainage patterns (Lemieux et al., 2008), various recharge rates due to changes in vegetation cover and permafrost extent (Ye et al., 2009), local sea-level fluctuations due to proglacial forebulge (Barnhardt et al., 1995), or the enhanced permeabilities associated with high hydraulic heads during glaciation periods (Boulton et al., 1995). The continuous deposition of outwash sediments during glacial retreat was not dynamically modeled, potentially affecting the evolution of hydraulic properties and aquifer connectivity (Müller et al., 2024). Additionally, our model does not account for isostatic rebound following ice sheet retreat, which may have influenced local hydraulic gradients and shoreline positions over time (Sanborn et al., 2025). These factors warrant further investigation through coupled stratigraphic and hydrogeological modeling in future studies.

Future climate change will likely affect passive OFG, as the rising sea level will intensify saltwater intrusion in offshore aquifers. Although active OFG may remain largely unaffected, local impacts could be seen along the PEI coast, where active continental shelf fresh water represents a valuable yet underutilized resource, though its development would be costly. Our study also has implications for estimates of SGD, particularly the often-overlooked offshore component. The results highlight how variations in OFG distribution and connectivity can influence the magnitude and spatial patterns of SGD. The SGD in the Gulf at the current sea level yielded by the model is shown in Fig. S7, with the high values covering the range of SGD rates measured from seepage meters installed along Cape Breton in Nova Scotia (Craddock et al., 2022). Increased SGD has the potential to impact not only shallow coastal ecosystems but also deeper marine environments. This flux could introduce nutrient-rich, chemically distinct groundwater to deeper ocean waters, altering biogeochemical cycles, oxygen levels, and overall ocean chemistry (Cheng et al., 2022; Wang et al., 2023; Yu et al., 2022). Such findings align with existing SGD literature (Lin et al.,2010; Paldor et al., 2020a, 2020b; Michael et al., 2016), which emphasizes the role of deep SGD as a significant, yet often underappreciated, component of the hydrological and marine system.

While our regional study provides valuable insights into the distribution and dynamics of OFG around PEI, determining whether OFG

should be utilized and at which specific locations as a freshwater source requires further exploratory studies focused on specific targets. Key concerns include the risk of over-extraction leading to seawater intrusion, irreversible depletion of the resource, and disruptions to marine and coastal ecosystems. Moreover, sustainable abstraction rates must be established to ensure long-term availability while minimizing environmental and economic costs. Addressing these concerns will require a comprehensive assessment of the aquifer systems, including high-resolution geophysical surveys, hydrogeological modeling, and ecological impact studies. The findings of this study highlight the importance of careful management and the need for more data and integrated water resource planning.

5. Conclusions

This study has investigated offshore freshened groundwater (OFG) patterns in formerly glaciated margins in the Gulf of St. Lawrence offshore PEI. The 3D geological model proved to be critical for evaluating the presence of OFG on the continental shelf, offering a more realistic representation of aquifer behavior in response to historical climate change. Our findings indicate that sub-ice-sheet recharge and meteoric recharge are the primary processes responsible for OFG emplacement. Anisotropy in geological formations facilitates present-day onshore-offshore aquifer connections, thereby promoting active recharge of OFG. The base-case model with unconsolidated marine sediment K_z of 10^{-7} m/s and thickness of 1 % aquifer thickness produced 57,950 km^3 of groundwater with a salinity lower than 1 g/L. An order-of-magnitude decrease and increase in K_z respectively yielded 95.9 % and 102.3 % OFG volume compared to the base case. When unconsolidated marine sediment thickness is 0.4 % and 4 % of the aquifer thickness, the OFG generated by the model is 55,748 km^3 and 62,784 km^3. The anisotropy value of 100 for both unconsolidated marine sediment and aquifer caused an OFG volume of 62,323 km^3 (107.6 % of the base case). All simulation results show completely freshened groundwater in offshore aquifers. The hydraulic connection between onshore and offshore aquifers is strengthened by decreasing hydraulic conductivity and increasing thickness of unconsolidated marine sediments, greater anisotropy, and the presence of interlayered aquitards. In contrast, increased hydraulic conductivity and decreased thickness of unconsolidated marine sediments, and reduced anisotropy weaken this connection and cause the OFG system to be passive. Current simulations are limited by the availability of measured data, simplified glacial boundary conditions, and assumptions in recharge estimation. Despite these constraints, our results are broadly relevant to understanding OFG systems in other glaciated and sedimentary continental margins worldwide. This work underscores the importance of historical reconstructions for predicting the vulnerability and sustainability of OFG in the face of climate change, coastal development, and future offshore resource exploitation. These findings provide critical insights into the environmental implications of OFG presence and how variations in OFG distribution and connectivity can influence the magnitude and spatial patterns of submarine groundwater discharge in deeper marine environments.

CRediT authorship contribution statement

Shengchao Yu: Writing – review & editing, Writing – original draft, Software, Methodology, Investigation, Formal analysis, Conceptualization. **Barret L. Kurylyk:** Writing – review & editing, Supervision, Resources, Methodology, Funding acquisition, Conceptualization. **Holly A. Michael:** Writing – review & editing, Supervision, Resources, Methodology, Funding acquisition, Conceptualization. **Vittorio Maselli:** Writing – review & editing, Resources, Project administration, Funding acquisition, Data curation. **Mladen R. Nedimović:** Writing – review & editing, Resources, Project administration, Funding acquisition, Data curation. **Irena Schulten:** Writing – review & editing, Visualization, Investigation. **Fernando Córdoba-Ramírez:** Writing – review & editing, Visualization, Investigation.

Declaration of competing interest

The authors declare that they have no known competing financial interests or personal relationships that could have appeared to influence the work reported in this paper.

Acknowledgments

Funding support was primarily from the Ocean Frontier Institute through an award from the Canada First Research Excellence Fund (CFREF). We are also grateful for the support provided by the Canada Research Chairs program to BK. We would like to acknowledge Aquanty for provision of the HydroGeoSphere software and technical support. Advanced computing resources were provided by the Digital Research Alliance of Canada, the organization responsible for digital research infrastructure in Canada, and ACENET, the regional partner in Atlantic Canada. We are grateful to the editor, associate editor, and three anonymous reviewers for their constructive comments that improved the quality of this paper.

Appendix A. Supplementary data

Supplementary data to this article can be found online at https://doi.org/10.1016/j.jhydrol.2025.134553.

Data availability

Model results will be made available on request.

References

Aeschbach-Hertig, W., Gleeson, T., 2012. Regional strategies for the accelerating global problem of groundwater depletion. Nat. Geosci. 5 (12), 853–861. https://doi.org/10.1038/ngeo1617.

Aquanty, 2022. HydroGeoSphere: A Three-Dimensional Numerical Model Describing Fully-integrated Subsurface and Surface Flow and Solute Transport. Aquanty, Waterloo, ON, Canada https://www.aquanty.com/hgs-download.

Anderson, M.P., 1989. Hydrogeologic facies models to delineate large-scale spatial trends in glacial and glaciofluvial sediments. Geol. Soc. Am. Bull. 101 (4), 501–511. https://doi.org/10.1130/0016-7606(1989)101<0501:HFMTDL>2.3.CO;2.

Atkinson, E.A., Durling, P.W., Kublik, K., Lister, C.J., King, H.M., Kung, L.E., Jassim, Y., McCarthy, W.M., Hayward, N., 2020. Qualitative petroleum resource assessment of the Magdalen Basin in the Gulf of St. Lawrence; Quebec, Prince Edward Island, New Brunswick, Nova Scotia, and Newfoundland and Labrador. Geological Survey of Canada, Open File, 8556, 109. https://doi.org/10.4095/321856.

Barnhardt, W.A., Roland Gehrels, W., Kelley, J.T., 1995. Late Quaternary relative sea-level change in the western Gulf of Maine: evidence for a migrating glacial forebulge. Geology 23 (4), 317–320. https://doi.org/10.1130/0091-7613(1995)023<0317:LQRSLC>2.3.CO;2.

Barss, M.S., Bujak, J.P., Williams, G.L., 1979. Palynological zonation and correlation of sixty-seven wells, eastern Canada (Vol. 78). Geological Survey of Canada, Paper, 78-24, 118. https://doi.org/10.4095/104894.

Boulton, G.S., Caban, P.E., Van Gijssel, K., 1995. Groundwater flow beneath ice sheets: Part I—Large scale patterns. Quat. Sci. Rev. 14 (6), 545–562. https://doi.org/10.1016/0277-3791(95)00039-R.

Cantelon, J.A., Kurylyk, B.L., 2024. Storm surge, seawater flooding, and sea-level rise paradoxically drive fresh surface water expansion. Environ. Res. Lett. 19 (12), 124038. https://doi.org/10.1088/1748-9326/ad8bdf.

Cheng, K.H., Luo, X., Jiao, J.J., Yu, S., 2022. Delineating E. coli occurrence and transport in the sandy beach groundwater system by radon-222. J. Hazard. Mater. 431, 128618. https://doi.org/10.1016/j.jhazmat.2022.128618.

Christian, H.A., 1993. June. In situ measurement of consolidation and permeability of soft marine sediments. In: In Proceedings of the 4th Canadian Conference on Marine Geotechnical Engineering, St. John's, Nfld, pp. 28–30.

Cohen, D., Person, M., Wang, P., Gable, C.W., Hutchinson, D., Marksamer, A., Dugan, B., Kooi, H., Groen, K., Lizarralde, D., Evans, R.L., 2010. Origin and extent of fresh paleowaters on the Atlantic continental shelf, USA. Groundwater 48 (1), 143–158. https://doi.org/10.1111/j.1745-6584.2009.00627.x.

Craddock, R.D., Kennedy, G.W., Jamieson, R.C., Keizer, J., Mohammed, A.A., Kurylyk, B. L., 2022. Assessment of groundwater discharge pathways in a till-dominated coastal aquifer. J. Hydrol.: Reg. Stud. 44, 101205. https://doi.org/10.1016/j.ejrh.2022.101205.

De Biase, M., Chidichimo, F., Thomas, A.T., Micallef, A., 2024. Limited role of present-day onshore freshwater recharge in the emplacement of offshore freshened groundwater in the Canterbury Bight, New Zealand. N. Z. J. Geol. Geophys. 1–15. https://doi.org/10.1080/00288306.2024.2387642.

Edmunds, W.M., Milne, C.J., (Eds.), 2001. Palaeowaters in coastal Europe: Evolution of groundwater since the Late Pleistocene. London: Geological Society of London, 289–311. https://doi.org/10.1144/GSL.SP.2001.189.01.19.

Ewing, M., Carpenter, G., Windisch, C., Ewing, J., 1973. Sediment distribution in the oceans: the Atlantic. Geol. Soc. Am. Bull. 84 (1), 71–88. https://doi.org/10.1130/0016-7606(1973)84<71:SDITOT>2.0.CO;2.

Faghih, Z., Haroon, A., Jegen, M., Gehrmann, R., Schwalenberg, K., Micallef, A., Dettmer, J., Berndt, C., Mountjoy, J., Weymer, B.A., 2024. Characterizing offshore freshened groundwater salinity patterns using trans-dimensional Bayesian inversion of controlled source electromagnetic data: a case study from the Canterbury Bight, New Zealand. Water Resour. Res. 60 (3), e2023WR035714. https://doi.org/10.1029/2023WR035714.

Frind, E.O., 1982. Simulation of long-term transient density-dependent transport in groundwater. Adv. Water Resour. 5 (2), 73–88. https://doi.org/10.1016/0309-1708(82)90049-5.

GEBCO, 2022. Gridded bathymetry data (general bathymetric chart of the oceans). British Oceanographic Data Centre (BODC). Available online at https://www.gebco.net/data_and_products/gridded_bathymetry_data/ (Accessed on March 2, 2023).

Gibling, M.R., Culshaw, N., Pascucci, V., Waldron, J.W.F., Rygel, M.C., 2019. The Maritimes Basin of Atlantic Canada: Basin creation and destruction during the Paleozoic assembly of Pangea. In: In the Sedimentary Basins of the United States and Canada. Elsevier, pp. 267–314. https://doi.org/10.1016/B978-0-444-63895-3.00006-1.

Giles, P.S., Utting, J., 1999. Maritimes basin stratigraphy, Prince Edward Island and adjacent Gulf of St. Lawrence. Natural Resources Canada, Geological Survey of Canada, Open File 3732. https://doi.org/10.4095/210469.

Gleeson, T., Befus, K.M., Jasechko, S., Luijendijk, E., Cardenas, M.B., 2016. The global volume and distribution of modern groundwater. Nat. Geosci. 9 (2), 161–167. https://doi.org/10.1038/ngeo2590.

Gleeson, T., Wada, Y., Bierkens, M.F., Van Beek, L.P., 2012. Water balance of global aquifers revealed by groundwater footprint. Nature 488 (7410), 197–200. https://doi.org/10.1038/nature11295.

Grant, A.C., Moir, P.N., 1992. Observations on coalbed methane potential, Prince Edward Island. Geol. Surv. Can. Pap. 92–1E, 269–278. https://doi.org/10.4095/133581.

Guimond, J.A., Michael, H.A., 2021. Effects of marsh migration on flooding, saltwater intrusion, and crop yield in coastal agricultural land subject to storm surge inundation. Water Resour. Res. 57 (2), e2020WR028326. https://doi.org/10.1029/2020WR028326.

Haroon, A., Micallef, A., Jegen, M., Schwalenberg, K., Karstens, J., Berndt, C., Garcia, X., Kühn, M., Rizzo, E., Fusi, N.C., Ahaneku, C.V., 2021. Electrical resistivity anomalies offshore a carbonate coastline: evidence for freshened groundwater? Geophys. Res. Lett. 48 (14), e2020GL091909. https://doi.org/10.1029/2020GL091909.

Hesse, R., Harrison, W.E., 1981. Gas hydrates (clathrates) causing pore-water freshening and oxygen isotope fractionation in deep-water sedimentary sections of terrigenous continental margins. Earth Planet. Sci. Lett. 55 (3), 453–462. https://doi.org/10.1016/0012-821X(81)90172-2.

Hong, W.L., Lepland, A., Himmler, T., Kim, J.H., Chand, S., Sahy, D., Solomon, E.A., Rae, J.W., Martma, T., Nam, S.I., Knies, J., 2019. Discharge of meteoric water in the eastern Norwegian Sea since the last glacial period. Geophys. Res. Lett. 46 (14), 8194–8204. https://doi.org/10.1029/2019GL084237.

Jiang, Y., Nishimura, P., van den Heuvel, M.R., MacQuarrie, K.T., Crane, C.S., Xing, Z., Raymond, B.G., Thompson, B.L., 2015. Modeling land-based nitrogen loads from groundwater-dominated agricultural watersheds to estuaries to inform nutrient reduction planning. J. Hydrol. 529, 213–230. https://doi.org/10.1016/j.jhydrol.2015.07.033.

Jiang, Y., Somers, G., 2009. Modeling effects of nitrate from non-point sources on groundwater quality in an agricultural watershed in Prince Edward Island, Canada. Hydrogeol. J. 17 (3), 707. https://doi.org/10.1007/s10040-008-0390-2.

Jiang, Y., Somers, G., Mutch, J., 2004. Application of numerical modeling to groundwater assessment and management in Prince Edward Island. In Proceedings of the 57th Canadian Geotechnical Conference, 57, 2–9.

Josenhans, H.W., Zevenhuizen, J., 1993. Quaternary sediment maps of the Gulf of St. Lawrence. Geol. Surv. Canada, Open File 2700. https://doi.org/10.4095/184204.

Keating, E.H., Robinson, B.A., Vesselinov, V.V., 2005. Development and application of numerical models to estimate fluxes through the regional aquifer beneath the Pajarito Plateau. Vadose Zone J. 4 (3), 653–671. https://doi.org/10.2136/vzj2004.0101.

Knight, A.C., Werner, A.D., Morgan, L.K., 2018. The onshore influence of offshore fresh groundwater. J. Hydrol. 561, 724–736. https://doi.org/10.1016/j.jhydrol.2018.03.028.

Kreyns, P., Geng, X., Michael, H.A., 2020. The influence of connected heterogeneity on groundwater flow and salinity distributions in coastal volcanic aquifers. J. Hydrol. 586, 124863. https://doi.org/10.1016/j.jhydrol.2020.124863.

Kwong, H.T., Jiao, J.J., 2016. Hydrochemical reactions and origin of offshore relatively fresh pore water from core samples in Hong Kong. J. Hydrol. 537, 283–296. https://doi.org/10.1016/j.jhydrol.2016.03.050.

Lemieux, J.M., Sudicky, E.A., Peltier, W.R., Tarasov, L., 2008. Simulating the impact of glaciations on continental groundwater flow systems: 1. Relevant processes and model formulation. J. Geophys. Res. Earth 113 (F3). https://doi.org/10.1029/2007JF000928.

LeRoux, N.K., Frey, S.K., Lapen, D.R., Guimond, J.A., Kurylyk, B.L., 2023. Mega-tidal and surface flooding controls on coastal groundwater and saltwater intrusion within agricultural dikelands. Water Resour. Res. 59 (11), e2023WR035054. https://doi.org/10.1029/2023WR035054.

Lin, I.T., Wang, C.H., You, C.F., Lin, S., Huang, K.F., Chen, Y.G., 2010. Deep submarine groundwater discharge indicated by tracers of oxygen, strontium isotopes and barium content in the Pingtung coastal zone, southern Taiwan. Mar. Chem. 122 (1–4), 51–58. https://doi.org/10.1016/j.marchem.2010.08.007.

Marshall, S.J., Clarke, G.K., 1999. Modeling North American freshwater runoff through the last glacial cycle. Quat. Res. 52 (3), 300–315. https://doi.org/10.1006/qres.1999.2079.

Maselli, V., 2022. Preliminary results from the first study for offshore groundwater exploration in Atlantic Canada. In Barr, S., GAC-MAC-IAH-CNC-CSPG 2022 Halifax Meeting: Abstracts, Volume 45. Geoscience Canada, 49(2), 59–226. https://doi.org/10.12789/geocanj.2022.49.188.

Micallef, A., Person, M., Berndt, C., Bertoni, C., Cohen, D., Dugan, B., Evans, R., Haroon, A., Hensen, C., Jegen, M., Key, K., 2021. Offshore freshened groundwater in continental margins. Rev. Geophys. 59 (1), e2020RG000706. https://doi.org/10.1029/2020RG000706.

Micallef, A., Person, M., Haroon, A., Weymer, B.A., Jegen, M., Schwalenberg, K., Faghih, Z., Duan, S., Cohen, D., Mountjoy, J.J., Woelz, S., 2020. 3D characterisation and quantification of an offshore freshened groundwater system in the Canterbury Bight. Nat. Commun. 11 (1), 1372. https://doi.org/10.1038/s41467-020-14770-7.

Michael, H.A., Scott, K.C., Koneshloo, M., Yu, X., Khan, M.R., Li, K., 2016. Geologic influence on groundwater salinity drives large seawater circulation through the continental shelf. Geophys. Res. Lett. 43 (20), 10–782. https://doi.org/10.1002/2016GL070863.

Michael, H.A., Voss, C.I., 2009a. Estimation of regional-scale groundwater flow properties in the Bengal Basin of India and Bangladesh. Hydrgeol. J. 17 (6), 1329–1346. https://doi.org/10.1007/s10040-009-0443-1.

Michael, H.A., Voss, C.I., 2009b. Controls on groundwater flow in the Bengal Basin of India and Bangladesh: regional modeling analysis. Hydrgeol. J. 17 (7), 1561–1577. https://doi.org/10.1007/s10040-008-0429-4.

Milliman, J.D., Emery, K.O., 1968. Sea levels during the past 35,000 years. Science 162 (3858), 1121–1123. https://doi.org/10.1126/science.162.3858.1121.

Morgan, L.K., Mountjoy, J.J., 2022. Likelihood of offshore freshened groundwater in New Zealand. Hydrgeol. J. 30 (7), 2013–2026. https://doi.org/10.1007/s10040-022-02525-1.

Morgan, L.K., Werner, A.D., Patterson, A.E., 2018. A conceptual study of offshore fresh groundwater behaviour in the Perth Basin (Australia): Modern salinity trends in a prehistoric context. J. Hydrol.: Reg. Stud. 19, 318–334. https://doi.org/10.1016/j.ejrh.2018.10.002.

Müller, T., Roncoroni, M., Mancini, D., Lane, S.N., Schaefli, B., 2024. Current and future roles of meltwater–groundwater dynamics in a proglacial Alpine outwash plain. Hydrol. Earth Syst. Sci. 28 (4), 735–759. https://doi.org/10.5194/hess-28-735-2024.

Mulligan, A.E., Evans, R.L., Lizarralde, D., 2007. The role of paleochannels in groundwater/seawater exchange. J. Hydrol. 335 (3–4), 313–329. https://doi.org/10.1016/j.jhydrol.2006.11.025.

Natural Resources and Renewables, 2006. Enhanced digital elevation model. Department of Natural Resources and Renewables. Geoscience & Mines Branch.

Oliver, A.C., Kurylyk, B.L., Johnston, L.H., LeRoux, N.K., Somers, L.D., Jamieson, R.C., 2024. Impacts of climate change and best management practices on nitrate loading to a eutrophic coastal lagoon. Front. Environ. Sci. 12, 1468869. https://doi.org/10.3389/fenvs.2024.1468869.

Paldor, A., Aharonov, E., Katz, O., 2020a. Thermo-haline circulations in subsea confined aquifers produce saline, steady-state deep submarine groundwater discharge. J. Hydrol. 580, 124276. https://doi.org/10.1016/j.jhydrol.2019.124276.

Paldor, A., Bertoni, C., Penny, B., Michael, H.A., 2024. Offshore freshened groundwater reservoirs controlled by submarine faults with a complex dependency on antecedent hydrogeological conditions. Sci. Total Environ. 952, 175834. https://doi.org/10.1016/j.scitotenv.2024.175834.

Paldor, A., Michael, H.A., 2021. Storm surges cause simultaneous salinization and freshening of coastal aquifers, exacerbated by climate change. Water Resour. Res. 57 (5), e2020WR029213. https://doi.org/10.1029/2020WR029213.

Paldor, A., Katz, O., Aharonov, E., Weinstein, Y., Roditi-Elasar, M., Lazar, A., Lazar, B., 2020b. Deep submarine groundwater discharge—evidence from Achziv submarine canyon at the exposure of the Judea group confined aquifer, Eastern Mediterranean. J. Geophys. Res. Oceans 125 (1), e2019JC015435. https://doi.org/10.1029/2019JC015435.

Paradis, D., Ballard, J., Savard, M.M., Lefebvre, R., Jiang, Y., Somers, G.H., Liao, S., Rivard, C., 2006. October. Impact of agricultural activities on nitrates in ground and surface water in the Wilmot Watershed, PEI, Canada. In: In 59th Canadian Geotechnical Conference and the 7th Joint CGS/IAH-CNC Conference, Vancouver, pp. 1–4.

Paradis, D., Vigneault, H., Lefebvre, R., Savard, M.M., Ballard, J.M., Qian, B., 2016. Groundwater nitrate concentration evolution under climate change and agricultural adaptation scenarios: Prince Edward Island, Canada. Earth Syst. Dynamics 7 (1), 183–202. https://doi.org/10.5194/esd-7-183-2016.

Pavlovskii, I., Jiang, Y., Danielescu, S., Kurylyk, B.L., 2023. Influence of precipitation event magnitude on baseflow and coastal nitrate export for Prince Edward Island, Canada. Hydrol. Processes 37 (5), e14892. https://doi.org/10.1002/hyp.14892.

Person, M., Dugan, B., Swenson, J.B., Urbano, L., Stott, C., Taylor, J., Willett, M., 2003. Pleistocene hydrogeology of the Atlantic continental shelf, New England. Geol. Soc. Am. Bull. 115 (11), 1324–1343. https://doi.org/10.1130/B25285.1.

Person, M., Marksamer, A., Dugan, B., Sauer, P.E., Brown, K., Bish, D., Licht, K.J., Willett, M., 2012. Use of a vertical δ18O profile to constrain hydraulic properties and recharge rates across a glacio-lacustrine unit, Nantucket Island, Massachusetts, USA. Hydrgeol. J. 20 (2), 325–336. https://doi.org/10.1007/s10040-011-0795-1.

Person, M., McIntosh, J., Bense, V., Remenda, V.H., 2007. Pleistocene hydrology of North America: the role of ice sheets in reorganizing groundwater flow systems. Rev. Geophys. 45 (3). https://doi.org/10.1029/2006RG000206.

Person, M., Wilson, J.L., Morrow, N., Post, V.E., 2017. Continental-shelf freshwater water resources and improved oil recovery by low-salinity waterflooding. AAPG Bull. 101 (1), 1–18. https://doi.org/10.1306/05241615143.

Post, V.E., Groen, J., Kooi, H., Person, M., Ge, S., Edmunds, W.M., 2013. Offshore fresh groundwater reserves as a global phenomenon. Nature 504 (7478), 71–78. https://doi.org/10.1306/05241615143.

Rehill, T.A., 1996. Late Carboniferous nonmarine sequence stratigraphy and petroleum geology of the central Maritimes Basin, eastern Canada. Dalhousie University PhD Thesis. http://hdl.handle.net/10222/55138.

Rivera, A. et Nastev, M. (2005). Overview of the groundwater resources of Canada. In Sahuquillo, A., Capilla, J., Martínez-Cortina, L. and Sánchez-Vila, X. (Eds), Groundwater intensive use. 157-165.

Sanborn, L.H., Pico, T., Donnelly, J.P., Perron, J.T., 2025. Glacial isostatic adjustment shifted early Holocene river hydrology in Maine, USA. Geology 53 (5), 446–450. https://doi.org/10.1130/G52822.1.

Savard, M.M., Somers, G., Paradis, D., van Bochove, E., Vigneault, H., Lefebvre, R., Thériault, G., De Jong, R., Jiang, Y., Qiang, B., Ballard, J.M., 2007. Consequences of climatic changes on contamination of drinking water by nitrate on Prince Edward Island. Natural Resources Canada, Canada, p. 61.

Schulten, I., Giona Bucci, M., Klein, J., 2022. Gravity coring. In Hölz, S., 2022. Groundwater resources offshore Prince Edward Island, Canada Cruise No. MSM103, 12.9.–15.11. 2021 Emden (Germany)–Halifax (Canada)–Emden (Germany); PRINCE. Bonn, Germany. https://doi.org/10.48433/cr_msm103.

Shaw, J., Gareau, P., Courtney, R.C., 2002. Palaeogeography of Atlantic Canada 13–0 kyr. Quat. Sci. Rev. 21 (16–17), 1861–1878. https://doi.org/10.1016/S0277-3791(02)00004-5.

Shaw, J., Piper, D.J.W., Fader, G.B.J., King, E.L., Todd, B.J., Bell, T., Batterson, M.J., Liverman, D.G.E., 2006. A conceptual model of the deglaciation of Atlantic Canada. Quat. Sci. Rev. 25 (17–18), 2059–2081. https://doi.org/10.1016/j.quascirev.2006.03.002.

Sheng, C., Jiao, J.J., Luo, X., Zuo, J., Jia, L., Cao, J., 2023. Offshore freshened groundwater in the Pearl River estuary and shelf as a significant water resource. Nat. Commun. 14 (1), 3781. https://doi.org/10.1038/s41467-023-39507-0.

Sheng, C., Jiao, J.J., Zhang, J., Yao, Y., Luo, X., Yu, S., Ni, Y., Wang, S., Mao, R., Yang, T., Zhan, L., 2024. Evolution of groundwater system in the Pearl River Delta and its adjacent shelf since the late Pleistocene. Sci. Adv. 10 (15), eadn3924. https://doi.org/10.1126/sciadv.adn3924.

Solórzano-Rivas, S.C., Werner, A.D., 2018. On the representation of subsea aquitards in models of offshore fresh groundwater. Adv. Water Resour. 112, 283–294. https://doi.org/10.1016/j.advwatres.2017.11.025.

Stanic, S., LeRoux, N.K., Paldor, A., Mohammed, A.A., Michael, H.A., Kurylyk, B.L., 2024. Saltwater intrusion into a confined island aquifer driven by erosion, changing recharge, sea-level rise, and coastal flooding. Water Resour. Res. 60 (1), e2023WR036394. https://doi.org/10.1029/2023WR036394.

Strassberg, G., Jones, N.L., Maidment, D.R., 2011. Arc Hydro Groundwater. ESRI Press, Redlands, California, pp. 14–30.

Thomas, A.T., Reiche, S., Riedel, M., Clauser, C., 2019. The fate of submarine fresh groundwater reservoirs at the New Jersey shelf, USA. Hydrgeol. J. 27 (7), 2673–2694. https://doi.org/10.1007/s10040-019-01997-y.

Tucholke, B.E., Houtz, R.E., Ludwig, W.J., 1982. Sediment thickness and depth to basement in western North Atlantic Ocean basin. AAPG Bull. 66 (9), 1384–1395. https://doi.org/10.1306/03B5A7AA-16D1-11D7-8645000102C1865D.

Vacchi, M., Engelhart, S.E., Nikitina, D., Ashe, E.L., Peltier, W.R., Roy, K., Kopp, R.E., Horton, B.P., 2018. Postglacial relative sea-level histories along the eastern Canadian coastline. Quat. Sci. Rev. 201, 124–146. https://doi.org/10.1016/j.quascirev.2018.09.043.

Varma, S., Michael, K., 2012. Impact of multi-purpose aquifer utilisation on a variable-density groundwater flow system in the Gippsland Basin, Australia. Hydrogeol. J. 20 (1), 119. https://doi.org/10.1007/s10040-011-0800-8.

Voss, C.I., Souza, W.R., 1987. Variable density flow and solute transport simulation of regional aquifers containing a narrow freshwater-saltwater transition zone. Water Resour. Res. 23 (10), 1851–1866. https://doi.org/10.1029/WR023i010p01851.

Waelbroeck, C., Labeyrie, L., Michel, E., Duplessy, J.C., Mcmanus, J.F., Lambeck, K., Balbon, E., Labracherie, M., 2002. Sea-level and deep water temperature changes derived from benthic foraminifera isotopic records. Quat. Sci. Rev. 21 (1–3), 295–305. https://doi.org/10.1016/S0277-3791(01)00101-9.

Wang, Q., Tang, G., Jiang, S., Wang, X., Xiao, K., Yu, S., Cai, P., Kuang, X., Li, H., 2023. Tracing terrestrial groundwater discharge and porewater exchange derived dissolved carbon export in a tropical estuary using multiple isotopes. J. Hydrol. 622, 129648. https://doi.org/10.1016/j.jhydrol.2023.129648.

Williamson, A.K., Grubb, H.F. and Weiss, J.S., 1990. Ground-water flow in the Gulf Coast aquifer systems, south central United States: a preliminary analysis. US Geological Survey, Department of the Interior, 89, 4071. https://doi.org/10.3133/wri894071.

Yang, J., Graf, T., Ptak, T., 2015. Sea level rise and storm surge effects in a coastal heterogeneous aquifer: a 2D modelling study in northern Germany. Grundwasser 20 (1), 39–51. https://doi.org/10.1007/s00767-014-0279-z.

Ye, B., Yang, D., Zhang, Z., Kane, D.L., 2009. Variation of hydrological regime with permafrost coverage over Lena Basin in Siberia. J. Geophys. Res. Atmos. 114. https://doi.org/10.1029/2008JD010537.

Yu, S., Jiao, J.J., Luo, X., Li, H., Wang, X., Wang, Q., Yao, M., Guo, Y., Deng, Z., Zuo, J., 2023a. Vertical leaching of paleo-saltwater in a coastal aquifer–aquitard system of the Pearl River Delta. J. Hydrol. 626, 130168. https://doi.org/10.1016/j.jhydrol.2023.130168.

Yu, S., Jiao, J.J., Luo, X., Li, H., Wang, X., Zhang, X., Yao, M., Zuo, J., Liang, W., Lu, M., 2023b. Evolutionary history of the groundwater system in the Pearl River Delta (China) during the Holocene. Geology 51 (5), 481–485. https://doi.org/10.1130/G50888.1.

Yu, S., Zhang, X., Li, H., Wang, X., Wang, C., Kuang, X., 2022. Analytical study for wave-induced submarine groundwater discharge in subtidal zone. J. Hydrol. 612, 128219. https://doi.org/10.1016/j.jhydrol.2022.128219.

Yu, X., Yang, J., Graf, T., Koneshloo, M., O'Neal, M.A., Michael, H.A., 2016. Impact of topography on groundwater salinization due to ocean surge inundation. Water Resour. Res. 52 (8), 5794–5812. https://doi.org/10.1002/2016WR018814.

Yu, X., Michael, H.A., 2019. Offshore pumping impacts onshore groundwater resources and land subsidence. Geophys. Res. Lett. 46 (5), 2553–2562. https://doi.org/10.1029/2019GL081910.

Zamrsky, D., Karssenberg, M.E., Cohen, K.M., Bierkens, M.F., Oude Essink, G.H., 2020. Geological heterogeneity of coastal unconsolidated groundwater systems worldwide and its influence on offshore fresh groundwater occurrence. Front. Earth Sci. 7, 339. https://doi.org/10.3389/feart.2019.00339.